Chapter 5

Quantum information diode based on the magnonic crystal

5.1 Introduction

A diode is a device designated to support asymmetric transport. Nowadays, household electric appliances or advanced experimental scientific equipment are all inconceivable without extensive use of diodes. Diodes with a perfect rectification effect permit electrical current to flow in one direction only. The progress in nanotechnology and material science passes new demands to a new generation of diodes; futuristic nano-devices that can rectify either acoustic (sound waves), thermal phononic, or magnonic spin current transport. Nevertheless, we note that at the nano-scale, the rectification effect is never perfect, *i.e.,* backflow is permitted, but amplitudes of the front and backflows are different [198, 199, 200, 201, 202, 203, 204, 205, 206, 207, 208, 209, 210, 211]. In the present work, we propose an entirely new type of diode designed to rectify the quantum information current. We do believe that in the foreseeable future the quantum information diode (QID) has a perspective to become a benchmark of quantum information technologies.

The functionality of a QID relies on the use of magnonic crystals, *i.e.,* artificial media with a characteristic periodic lateral variation of magnetic properties. Similar to photonic crystals, magnonic crystals possess a band gap in the magnonic excitation spectrum. Therefore, spin waves with frequencies matching the band gap are not allowed to propagate through the magnonic crystals [85, 89, 212, 213, 214, 215, 216].

The essence of a magnonic transistor is an YIG strip with a periodic modulation of its thickness (magnonic crystal). The transistor is complemented by a source, a drain, and gate antennas. A gate antenna injects magnonic crystal magnons with a frequency ω_G matching the magnonic crystal band gap. Therefore, the gate magnons cannot leave the crystal and may reach a high density. Magnons emitted from a source with a wave vector $\mathbf{k}_s$ flowing towards the drain run into the magnonic crystal. The interaction between the source magnons and the magnonic crystal magnons is a four-magnon scattering process. The magnonic current emitted from the source attenuates in the magnonic crystal, and the weak signal reaches the drain due to the scattering. The relaxation process is swift if the following condition holds [89, 90]

$$k_s = \frac{m_0 \pi}{a_0}, \tag{5.1}$$

where m_0 is the integer, and a_0 is the crystal lattice constant. The magnons with wave vectors satisfying the Bragg conditions Eq. (5.1) will be resonantly scattered back, resulting in the generation of rejection bands in a spin-wave spectrum over which magnon propagation is entirely prohibited. Experimental verification of this effect is given in Ref. [89].

This chapter is organized as follows. In subsection 5.2.1, we briefly describe the proposed set-up for QID. In subsection 5.2.2, we will discuss a model of a 2D square lattice spin system. OTOC is defined in subsection 5.2.3, and rectification is defined in subsection 5.2.4. At last, we conclude the results in section 5.3

5.2 Result

5.2.1 Proposed set-up for QID

A pictorial representation of a QID is shown in Fig. 5.1. A magnonic crystal can be fabricated from an YIG film. Grooves can be deposited using a lithography procedure in a few nanometer steps, and for our purpose, we consider parallel lines in width of 1μm spaced with 10μm from each other. Therefore, the lattice constant, approximately $a_0 = 11\mu$m, *i. e.,* is much larger than the unit cell size $a = 10$nm used in our coarse-graining approach. Due to the capacity of our analytical calculations, we consider quantum spin chains of length about $N = 1000$ spins and the maximal distance between the spins $r_{ij} = d$ (in the units of a), $d = i - j = 40$. In what follows, we take $k(\omega)a \ll 1$. The mechanism of the QID is based on the effect of direction dependence of nonreciprocal magnons [217, 218, 219]. In the chiral spin systems, the absence of inversion symmetry causes a difference in dispersion relations of the left and right propagating magnons, *i. e.,* $\omega_{s,L}(\mathbf{k}) \neq \omega_{s,R}(-\mathbf{k})$. Due to the Dzyaloshinskii–Moriya interaction (DMI), magnons of the same frequency ω_s propagating in opposite directions have different wave vectors [220]: $a\,(k_s^+ - k_s^-) = D/J$, where J is the exchange constant, and D is the DMI constant. Therefore, if the condition Eq. (5.1) holds for the left propagating magnons, it is violated for the right propagating magnons and vice versa. These magnons propagating in different directions decay differently in the magnonic crystal. Without loss of generality, we assume that the right propagating magnons with k_s^+ satisfy the condition Eq. (5.1), and the current attenuates due to the scattering of source magnons by the gate magnons. The left propagating magnons k_s^- violate the condition Eq. (5.1), and the current flows without scattering. Thus, reversing the source and drain antenna's positions rectifies the current. Following ref. [89], we introduce a suppression rate of the source to drain the magnonic current $\xi(D) = 1 - n_D^+/n_D^-$, where $n_D^+ < n_D^-$ are densities of the drain magnons with and

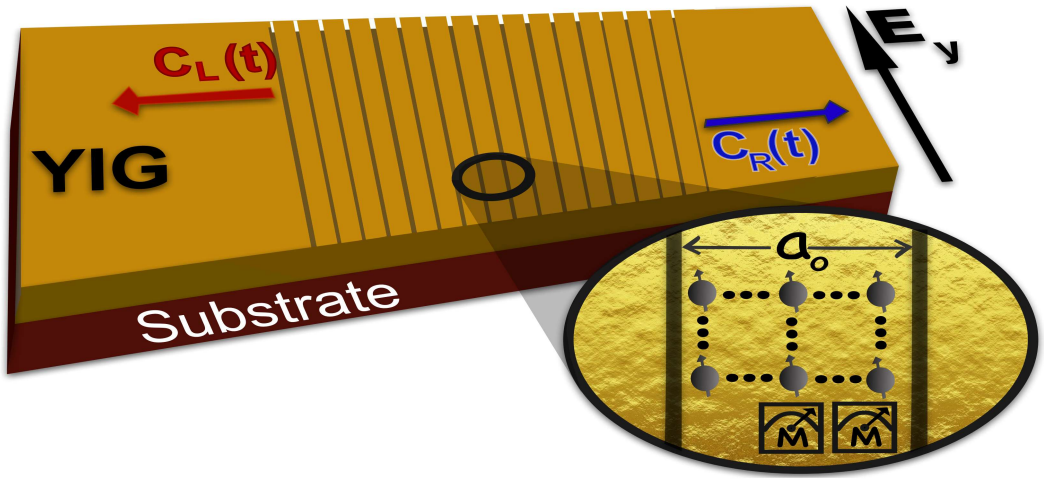

Fig. 5.1 Illustration of a quantum information diode: A plane of an YIG film with grooves orthogonal to the direction of the propagation of quantum information. In the middle of the QID, we pump extra magnons to excite the system. A quantum excitation propagates toward the left, and the right ends asymmetrically. To describe the propagation process of quantum information, we introduce the left and right OTOC $C_L(t)$ and $C_R(t)$. Because the left-right inversion is equivalent to $D \to -D$ meaning $E_y \to -E_y$, we can invert the left and right OTOCs by switching the applied external electric field.

without scattering. The parameter $\xi(D)$ is experimentally accessible, and it depends on a particular setup. Therefore, we take $\xi(D)$ as a free theory parameter. Multiferroic (MF) materials are considered as a good example of a system with broken inversion symmetry (see Refs.[221, 222, 223, 224, 225, 226, 227, 228, 229]) and references therein. MF properties of YIG are studied in ref. [230]. Moreover, in accordance with scanning tunneling microscopy experiments, a change of the spin direction at one edge of a chiral chain was experimentally probed by tens of nanometers away from the second edge [229].

5.2.2 Model

We consider a 2D square-lattice spin system with nearest-neighbor J_1 and the next nearest-neighbor J_2 coupling constants:

$$\hat{H} = J_1 \sum_{\langle n,m \rangle} \hat{\sigma}_n \hat{\sigma}_m + J_2 \sum_{\langle\langle n,m \rangle\rangle} \hat{\sigma}_n \hat{\sigma}_m - \mathbf{P} \cdot \mathbf{E}, \tag{5.2}$$

where $\langle n,m \rangle$, and $\langle\langle n,m \rangle\rangle$ indicate all the pairs with nearest-neighbor and next nearest-neighbor interactions, respectively. The last term in Eq. (5.2) describes a coupling of the ferroelectric polarization $\mathbf{P} = g_{\mathrm{ME}} \mathbf{e}^x_{i,i+1} \times (\hat{\sigma}_i \times \hat{\sigma}_{i+1})$ with an applied external electric field and mimics an effective Dzyaloshinskii–Moriya interaction term $D = E_y g_{\mathrm{ME}}$ breaking the left-right symmetry, where g_{ME} is the magneto-electric coupling constant. This can be written as

$$-\mathbf{P} \cdot \mathbf{E} = D \sum_n (\hat{\sigma}_n \times \hat{\sigma}_{n+1})_z. \tag{5.3}$$

Here we consider only the nearest neighbor DMI and only in one direction. As a consequence, the left-right inversion is equivalent to $D \to -D$, or $E_y \to -E_y$. The broken left-right inversion symmetry can be exploited in rectifying the information current by an electric field. More importantly, the procedure is experimentally feasible. We can diagonalize the Hamiltonian in Eq. (5.2) by using the Holstein-Primakoff transformation [231, 232, 233, 234] [See Appendix D-I for detailed derivation] as:

$$\begin{aligned}
&\hat{H} = \sum_{\vec{k}} \omega(\pm D, \mathbf{k}) \hat{a}^\dagger_{\vec{k}} \hat{a}_{\vec{k}},\ \omega(\pm D, \mathbf{k}) = \left(\omega(\vec{k}) \pm \omega_{DM}(\vec{k})\right),\ \ \omega_{DM}(\vec{k}) = D \sin(k_x a), \\
&\omega_k = 2J_1(1 - \gamma_{1,\mathbf{k}}) + 2J_2(1 - \gamma_{2,\mathbf{k}}),\ \gamma_{1,\mathbf{k}} = 1/2(\cos k_x + \cos k_y), \\
&\gamma_{2,\mathbf{k}} = 1/2(\cos(k_x + k_y) + \cos(k_x - k_y)).
\end{aligned} \tag{5.4}$$

Here $\pm D$ corresponds to the magnons propagating in opposite directions, and the sign change is equivalent to the electric field direction change. We note that a 1D character of

the DM term is ensured by the magnetoelectric effect [221] and to the electric field applied along the **y** axis.

The speed limit of information propagation is usually given in terms of Lieb-Robinson (LR) bound, defined for the Hamiltonians that are locally bounded and short-range interacting [235, 236, 237]. Since the Hamiltonian in Eq. (5.2) satisfies both conditions, the LR bound can be defined for the spin model. However, when we transform the Hamiltonian using Holstein-Primakoff bosons, we have to take extra care as the bosons are not locally bounded. To define LR bound, we take only a few noninteracting magnons and exclude the magnon-magnon interaction to truncate terms beyond quadratic operators. In a realistic experimental setting, low density of propagating magnons in YIG can easily be achieved by properly controlling the microwave antenna. In the case of low magnon density, the role of the magnon-magnon interaction between propagating magnons in YIG is negligible. Therefore, for YIG, we have a quadratic Hamiltonian, which is a precise approach in a low magnon density limit. Our discussion is valid for the experimental physical system [89], where magnons of YIG do not interact with each other, implying that there is no term in the Hamiltonian beyond quadratic. We can estimate LR bounds [238] defining the maximum group velocities of the left-right propagating magnons $v_g^{\pm}(\vec{k}) = \frac{\partial(\omega(\vec{k}) \pm \omega_{DM}(\vec{k}))}{\partial k}$. Taking into account the explicit form of the dispersion relations, we see that the maximal asymmetry is approximately equal to the DM constant, *i. e.,* $v_g^+(0) - v_g^-(0) \approx 2D$. We note that the effect of nonreciprocal magnons is already observed experimentally [239, 240, 241, 242, 243] but up to date, never discussed in the context of the quantum information theory.

We formulate the central interest question as follows: At $t = 0$, we act upon the spin $\hat{\sigma}_n$ to see how swiftly changes in the spin direction can be probed tens of sites away $d = n - m \gg 1$ and whether the forward and backward processes (, *i.e.,* probing for $\hat{\sigma}_m$ the outcome of the measurement done on $\hat{\sigma}_n$) are asymmetric or not. Due to the left-right asymmetry, the chiral spin channel may sustain a diode rectification effect when

transferring the quantum information from left to right and in the opposite direction. We note that our discussion about the left-right asymmetry of the quantum information flow is valid until the current reaches boundaries. Thus the upper limit of the time reads $t_{\max} = Na/v_g^{\pm}(\vec{k})$, where N is the size of the system.

5.2.3 Out-of-time-order correlator

Larkin and Ovchinnikov [19] introduced the concept of the out-of-time-ordered correlator (OTOC), and since then, OTOC has been seen as a diagnostic tool of quantum chaos. The concern of delocalizations in the quantum information theory (*i.e.,* the scrambling of quantum entanglement) was renewed only recently, see Refs. [14, 94, 97, 99, 133, 134, 244, 245, 246, 247] and references therein. We utilize the OTOC to characterize the left-right asymmetry of the quantum information flow and thus infer the rectification effect of a diode.

Let us consider two unitary operators $\hat{V}$ and $\hat{W}$ describing local perturbations to the chiral spin system Eq. (5.2), and the unitary time evolution of one of the operators $\hat{W}(t) = \exp(i\hat{H}t)\hat{W}(0)\exp(-i\hat{H}t)$. Then the OTOC is defined as

$$C(t) = \frac{1}{2}\left\langle \left[\hat{W}(t),\hat{V}(0)\right]^{\dagger}\left[\hat{W}(t),\hat{V}(0)\right]\right\rangle, \tag{5.5}$$

where parentheses $\langle\cdots\rangle$ denotes a quantum mechanical average over the propagated quantum state. Following the definition, the OTOC at the initial moment of time is zero $C(0) = 0$, provided that $[\hat{W}(0),\hat{V}(0)] = 0$. In particular, for the local unitary and Hermitian operators of our choice $\hat{W}_m^{\dagger}(t) \equiv \hat{\sigma}_m^z(t) = \hat{\eta}_m(t) = \exp(i\hat{H}t)\hat{\eta}_m\exp(-i\hat{H}t)$, and $\hat{V}_n^{\dagger} = \hat{\sigma}_n^z = \hat{\eta}_n$, where $\hat{\eta}_n = \hat{2}a_n^{\dagger}\hat{a}_n - 1$. The bosonic operators are related to the spin operators via $\sigma_n^- = 2a_n^{\dagger}$, $\sigma_n^+ = 2a_n$, $\sigma_n^z = 2a_n^{\dagger}a_n - 1$. In terms of the occupation number

operators, the OTOC is given as

$$C(t) = \frac{1}{2}\Big\{\langle\eta_n\eta_m(t)\eta_m(t)\eta_n\rangle + \langle\eta_m(t)\eta_n\eta_n\eta_m(t)\rangle - \langle\eta_m(t)\eta_n\eta_m(t)\eta_n\rangle - \langle\eta_n\eta_m(t)\eta_n\eta_m(t)\Big\}. \tag{5.6}$$

Indeed, the OTOC can be interpreted as the overlap of two wave functions, which are time evolved in two different ways for the same initial state $|\psi(0)\rangle$. The first wave function is obtained by perturbing the initial state at $t = 0$ with a local unitary operator $\hat{V}$, then evolved further under the unitary evolution operator $\hat{U} = \exp(-\mathrm{i}\hat{H}t)$ until time t. It is then perturbed at time t with a local unitary operator $\hat{W}$, and evolved backwards from t to $t = 0$ under $\hat{U^\dagger}$. Hence, the time evolved wave function is $|\psi(t)\rangle = \hat{U^\dagger}\hat{W}\hat{U}\hat{V}|\psi(0)\rangle = \hat{W}(t)\hat{V}|\psi(0)\rangle$. To get the second wave function, the order of the applied perturbations is permuted, *i. e.,* first $\hat{W}$ at t and then $\hat{V}$ at $t = 0$. Therefore, the second wave-function is $|\phi(t)\rangle = \hat{V}\hat{U^\dagger}\hat{W}\hat{U}|\psi(0)\rangle = \hat{V}\hat{W}(t)|\psi(0)\rangle$ and their overlap is equivalent to $F(t) = \langle\phi(t)|\psi(t)\rangle$. The OTOC is calculated from this overlap using $C(t) = 1 - \Re[F(t)]$. What breaks the time inversion symmetry for the OTOC is the permuted sequence of operators $\hat{W}$ and $\hat{V}$. However, in spin-lattice models with a preserved spatial inversion symmetry $\hat{\mathscr{P}}\hat{H} = \hat{H}$, the spatial inversion $\hat{\mathscr{P}}d(\hat{W},\hat{V}) = -d(\hat{W},\hat{V}) = d(\hat{V},\hat{W})$ can restore the permuted order between $\hat{V}$ and $\hat{W}$, where $d(\hat{W},\hat{V})$ denotes the distance between observables $\hat{W}$ and $\hat{V}$. Permuting just a single wave-function one finds $C(t) = 1 - \Re(\langle\phi(t)|\hat{\mathscr{P}}\hat{\mathscr{T}}|\psi(t)\rangle) = C(0)$. Thus, a scrambled quantum entanglement formally can be unscrambled by a spatial inversion. However, in chiral systems $\hat{\mathscr{P}}\hat{H} \neq \hat{H}$ and the unscrambling procedure fails.

Taking into account Eq. (5.4), we analyze quantum information scrambling along the **x** axis, *i. e.,* $\omega(\pm D,\mathbf{k}) = \omega(\pm D,k_x,0)$ and along the **y** axis, $\omega(0,\mathbf{k}) = \omega(0,0,k_y)$. It is easy to see that the quantum information flow along the **y** axis is symmetric, while along the **x** axis, it is asymmetric and depends on the sign of the DM constant, , *i.e.,* the flow along the **x** is different from $-\mathbf{x}$. Let us assume that Eq. (5.1) holds for right-moving magnons and is violated for left-moving magnons. Excited magnons with the same frequency and

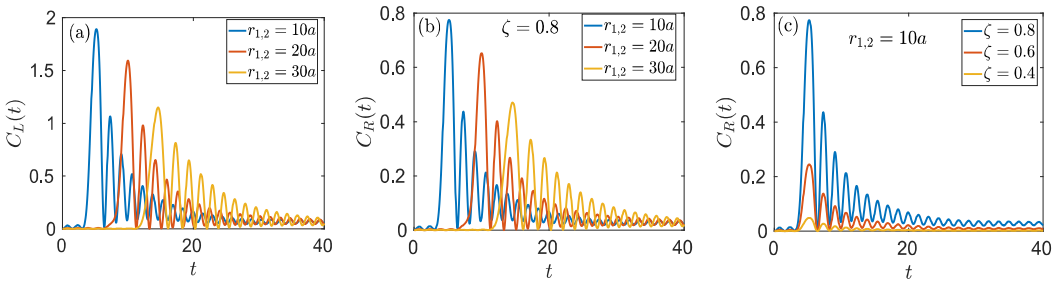

Fig. 5.2 **(a)** Left-OTOC and **(b)** Right-OTOC with time t (in the units of $1/J$) for different distances $r_{1,2} = 10a$, $20a$ and $30a$. **(c)** Right-OTOC with time for $r_{1,2} = 10a$ and suppression rates of the magnon current $\zeta = 0.8$, 0.6 and 0.4. Parameters are $N = 1000$, $D = J_1 = 2J_2 = 1$. Periodic boundary conditions are considered. The values of the parameters: $m_0 = 1$ to N, $a = 10^{-3}$ and $a_0 = 1$.

propagating into different directions have different wave vectors $\omega_s(D, k_s^+) = \omega_s(-D, k_s^-)$ where:

$$\omega_s\left(\pm D, k_s^{\pm}\right) = 2J_1(1 - 1/2\cos k_x^{\pm} a) + 2J_2(1 - \cos k_x^{\pm} a) \pm D \sin k_x^{\pm} a, \tag{5.7}$$

$k_{m_0 x}^+ = \frac{m_0 \pi}{a_0}$, $m_0 = \mathbb{N}$ and $k_{m_0 x}^-$ we find from the condition $\omega_s(D, k_s^+) = \omega_s(-D, k_s^-)$ leading to $k_{m_0 x}^- = k_{m_0 x}^+ + \frac{2}{a}\tan^{-1}\left(\frac{D}{J_1 + 2J_2}\right)$. Here we use shortened notations $\omega_{m_0} = \omega_s(D, k_s^+) = \omega_s(-D, k_s^-)$ and set dimensionless units $J_1 = 2J_2 \equiv J = 1$. We excite in the diode magnons of different frequencies $m_0 = [1, N]$. Considering Eq. (5.6), Eq. (5.7) and following Ref. [233] we obtain expressions for the left and right OTOCs $C_L(t)$ and $C_R(t)$. Those expressions and details of involved derivations are presented in Appendix D-II. In Fig. 5.2, $C_L(t)$ and $C_R(t)$ is shown for $|n^+ - m|$ and $|n^- - m|$ distant spins, respectively. $C_R(t)$ is independent of the separation between the spins; however, the decay amplitude varies due to the suppression coefficient ζ. In the case of the dominant attenuation by the gate magnons, the OTOC decreases significantly. The difference in C_L and C_R originated due to the asymmetry arising from the DMI term.

A high density of magnons can invalidate the assumption of a pure state or spin-wave approximation that works only for a low density of magnons. However, the key point

in our case is that one has to distinguish between two sorts of magnons, gate magnons and propagating nonreciprocal magnons. The density of the propagating magnons can be regulated in the experiment through a microwave antenna, and one can always ensure that their density is low enough. It is easy to regulate the density of the gate magnons, and an experimentally accessible method is discussed in Ref. [89].

We proposed a novel theoretical concept that can be directly realized with the experimentally feasible setup and particular material. There are several experimentally feasible protocols for measuring OTOC in the spin systems [101, 248]. According to these protocols, one needs to initialize the system into the fully polarized state, then apply quench and measure the expectation value of the first spin. All these steps are directly applicable to our setup from YIG. The fully polarized initial state can be obtained by switching on and off a strong magnetic field at a time moment $t = 0$. Quench, in our case, is performed by a microwave antenna which is an experimentally accessible device. Polarization of the initial spin can be measured through the STM tip. Overall our setup is the experimentally feasible setup studied in Ref. [89].

5.2.4 Rectification

Let us calculate the total amount of correlations transferred in opposite directions followed by the rectification coefficient, a function of the external electric field as $R = \frac{\int_0^\infty C_R(t)dt}{\int_0^\infty C_L(t)dt}$. We interpolate the suppression rate as a function of the DMI coefficient in the form $\zeta(D) \approx e^{-D/5}$. The coefficient $\zeta(D)$ mimics a scattering process of the drain magnons on the gate magnons [89]. In Fig. 5.3, we see the variation of the rectification coefficient as a function of D. The electric field has a direct and important role in rectification. In particular, DMI constant D depends on the electric field E_y as $D = E_y g_{ME}$, where g_{ME} is the magneto-electric coupling constant. In the case of zero electric fields, D will be zero, implying the absence of rectification effect $R = 1$. As the electric field increases, D also

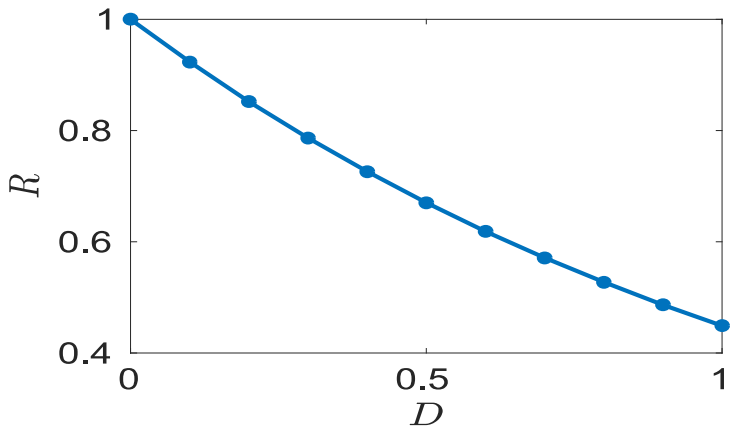

Fig. 5.3 Rectification coefficient R is plotted against DMI coefficient (D) for suppression rate $\zeta(D) \approx e^{-D/5}$. The parameters are $J_1 = 2J_2 = 1$, $N = 1000$, $r_{12} = 10a$, $a_0 = 1$ and $m_0 = 1$ to N.

increases linearly, and rectification decreases exponentially. A detailed study of the role of the electric field in DM has been done in Ref. [230].

5.3 Conclusions

We studied a quantum information flow in a spin quantum system. In particular, we proposed a quantum magnon diode based on YIG and magnonic crystal properties. The flow of magnons with wavelengths satisfying the Bragg conditions $k = m_0\pi/a_o$ is reflected from the grooves. Due to the absence of inversion symmetry in the system, left and right-propagating magnons have different dispersion relations and wave vectors. While for the right propagating magnons, the Bragg conditions hold, left magnons violate them, leading to an asymmetric flow of the quantum information.

We found that the strength of quantum correlations depends on the distance between spins and time. The OTOC for the spins separated by longer distance shows an inevitable delay in time, meaning that the quantum information flow has a finite "butterfly velocity." On the other hand, the OTOC amplitude becomes smaller at longer distances between

spins. The reason is that the initial amount of quantum information spreads among more spins. After the quantum information spreads over the whole system, which is pretty large ($N = 1000$ sites), the OTOC again becomes zero.

In the next chapter, we will summarise our complete results and discuss future plans that could be done on the basis of our previous work.